

IMPACT OF BOTTOM STRESS AND CURRENTS ON WAVE-CURRENT INTERACTIONS

Yin Baoshu^{1,3}, Will Perrie³, HouYijun¹, Lin Xiang^{1,2}, Cheng Minghua¹

¹Inst.of Oceanology, Chinese Academy of Sciences, Qingdao, PR China

²Graduate school, Chinese Academy of Sciences, Beijing, PR China

³Fisheries & Oceans Canada, Bedford Institute of Oceanography, Dartmouth, Nova Scotia , Canada

1. INTRODUCTION

Wave-current interactions are important for calculation of impacts on bed stress due to wind wave activity in the coastal region. This is important for a robust theoretical basis for sediment transport estimates, beach evolution calculations and concomitant processes related to the study of land-sea interactions in the coastal area. In recent years, there has been increased interest in developing models that can resolve the near-bed region, taking account of impacts due to near-bed turbulence related to wind-wave activity. However, how to calculate the bottom stress has become an important problem in understanding the processes that control and define wave-current interactions. At present, there are two widespread methods to calculate the bottom stress. One is called the integral method, given by Grant and Madsen (1979). The other is called the separation method, given by Christoffersen and Jonsson (1985).

Signell et al.(1990) included wave-current interaction effects in an idealized estuarine model and showed that they could influence the flow field. Davies et al.(1994) used a similar approach to examine the influence of enhancements in bed stress due to wave-current interactions upon the wind-induced circulation of the eastern Irish Sea. In this paper, a two-dimensional current model is coupled with a third generation shallow water wave model to examine the changes of bottom stress and current velocity due to wave-current interactions in the coastal region of the Bohai Sea.

2. HYDRODYNAMIC MODEL

2.1 Two-Dimensional Current Model

This model is motivated by a similar development by Fang and Cao (1990). A Cartesian coordinate system is assumed, with x and y coordinates directed to the east and north, respectively. The continuity and momentum equations are

$$\frac{\partial \zeta}{\partial t} + \frac{\partial}{\partial x} [(h + \zeta)u] + \frac{\partial}{\partial y} [(h + \zeta)v] = 0 \quad (1)$$

$$\frac{du}{dt} - fv = -g \frac{\partial \zeta}{\partial x} + \frac{1}{\rho} \frac{\tau_{ax} - \tau_{bx}}{h + \zeta} + A_x \left(\frac{\partial^2 u}{\partial x^2} + \frac{\partial^2 u}{\partial y^2} \right) \quad (2)$$

$$\frac{dv}{dt} + fu = -g \frac{\partial \zeta}{\partial y} + \frac{1}{\rho} \frac{\tau_{ay} - \tau_{by}}{h + \zeta} + A_y \left(\frac{\partial^2 v}{\partial x^2} + \frac{\partial^2 v}{\partial y^2} \right) \quad (3)$$

where (u, v) are the eastward and northward components of the depth-averaged velocity vector, respectively; t is time, f is the Coriolis parameter, A_x and A_y are the eddy viscosities; g is the gravitational acceleration, ρ is the density of sea water, $(h + \zeta)$ is the total depth (mean water + surface elevation), $\bar{\tau}_s = (\tau_x, \tau_y)$ is surface wind stress, and $\bar{\tau}_b = (\tau_{bx}, \tau_{by})$ is the bottom stress.

2.2 Initial and Boundary Conditions

We assume the initial conditions,

$$\zeta = u = v = 0 \quad (4)$$

and lateral boundary conditions, that the flow is zero normal to the solid boundary and along the open boundary

$$\zeta = \frac{P_b - P_o}{\rho g} + \sum f_i H_i \cos[\omega_i t + (v + u)_i - g_i]. \quad (5)$$

Here, P_o and P_b are the atmospheric pressures outside a storm and at the open boundary, ρ is the density of sea water, g is the gravitational acceleration, the ten tidal constituents are taken as K_1 , O_1 , P_1 , Q_1 , M_2 , S_2 , N_2 , K_2 , S_a , S_{sa} . The radian frequency is ω_i ; harmonic constants; H_i and g_i are the amplitude and phase angle of each constituent; f_i is the nodal factor of each constituent; $(v + u)_i$ is the initial phase and u_i is the nodal correction angle.

Surface wind stress is generally assumed to take the form

$$\bar{\tau}_s = \rho_a C_d |\bar{w}_{10}| \bar{w}_{10} \quad (6)$$

where ρ_a is the air density; C_d , is the surface aerodynamic drag coefficient and \bar{w}_{10} denotes wind velocity vector at 10m reference height. A wave-age dependent C_d formulation would assume the functional dependence of the HEXOS relation of Smith et al. (1992). However, in this study, we take a conventional approach, following Hsu (1986), and we assume that C_d takes the form

$$C_d = \lambda \left\{ \frac{0.4}{14.56 - 2 \ln |\bar{w}_{10}|} \right\}^2 \quad (7)$$

where λ is an adjustable coefficient depending on differing weather conditions (~ 1.1 for typhoons, ~ 1.0 for extra-tropical systems). When we don't consider wave-current interactions, bottom stress is assumed to be,

$$\bar{\tau}_b = \rho_w \gamma |\bar{u}| \bar{u}, \quad \gamma = \frac{ng}{c_z^2} \quad (8)$$

where c_z is the Chezy-Manning coefficient and \bar{u} is the current velocity vector.

According to the wave-current interaction model of Grant and Madsen (1979), in the form published by Signell et al (1990), a collinear flow implies that the total bed shear stress is given by:

$$\tau_T = \tau_c + \tau_w \quad (9)$$

where τ_c is an instantaneous current shear stress and τ_w is the maximum wave bed stress, as given by

$$\tau_w = \frac{1}{2} \rho f_w |U_0|^2 \quad (10)$$

where U_0 is the maximum near-bed wave orbital velocity, and f_w is the wave friction factor. The near-bed

wave orbital velocity is given by

$$U_0 = \frac{a_w \sigma}{\sinh kh} \quad (11)$$

where a_w is the wave amplitude, σ is wave frequency, and k is the wave number determined from the linear dispersion relation

$$\sigma^2 = (gk) \tanh(kh) . \quad (12)$$

The wave friction factor f_w can be readily computed from the semi-empirical expression of Jonsson and Carlsen (1976), based upon laboratory observations, This implies,

$$\frac{1}{4\sqrt{f_w}} + \log_{10} \left(\frac{1}{4\sqrt{f_w}} \right) = -0.08 + \log_{10} \left(\frac{A_b}{k_b} \right) \quad (13)$$

where $k_b = 30z_0$, and z_0 is the *bottom* roughness length and $A_b = U_0 / \sigma$.

If we assume that the current doesn't influence the wave field, the wave friction velocity is given by,

$$U_{*w} = \left(\frac{\tau_w}{\rho} \right)^{1/2} . \quad (14)$$

At initial time $t = 0$, an initial current friction factor f_c , excluding wind wave turbulence, is determined from

$$f_c = 2 \left[\frac{0.4}{\ln(30z_r / k_{bc})} \right]^2 \quad (15)$$

with k_{bc} taken as the Nikuradse roughness $k_{bc} = k_b = 30z_0$, and z_r was taken as 100 cm above the bed. Once f_c is determined, U_{*c} can be readily computed from

$$U_{*c} = \left(\frac{\tau_c}{\rho} \right)^{1/2} \quad (16)$$

where $\tau_c = \sqrt{F_B^2 + G_B^2}$ and F_B and G_B are given as

$$F_B = \frac{1}{2} f_c \rho u (u^2 + v^2)^{1/2} \quad (17)$$

$$G_B = \frac{1}{2} f_c \rho v (u^2 + v^2)^{1/2} . \quad (18)$$

The combined friction velocity U_{*cw} for waves and currents is given by

$$U_{*cw} = \left(U_{*c}^2 + U_{*w}^2 \right)^{1/2} . \quad (19)$$

The apparent bottom roughness k_{bc} felt by the current due to the presence of the waves is given by

$$k_{bc} = k_b \left(C_1 \frac{U_{*cw} A_b}{U_w k_b} \right)^\beta \quad (20)$$

with $C_1 = 24.0$, from Grant and Madsen (1979), and

$$\beta = 1 - \frac{U_{*c}}{U_{*cw}} \quad (21)$$

The value for k_{bc} is then used at the next time step to determine f_c , and hence the bed stress due to the wave field and the time-evolving viscosity field may be estimated,

$$\bar{\tau}_c = \frac{1}{2} \rho f_c |\bar{u}|^2 \bar{u} \quad (22)$$

2.2 Wave Model

The third generation shallow water wave model YWE-WAM used in this study is based on the action balance equation of WAMDI (1988). Source functions are taken directly from the standard WAM model, except for the dissipation due to depth-induced breaking, which is explicitly parameterized. The basic equations are

$$\frac{\partial N}{\partial t} + \nabla[(\bar{C}_g + \bar{u})N] + \frac{\partial}{\partial \sigma}[C_\sigma N] + \frac{\partial}{\partial \theta}(c_\theta N) = \frac{S}{\sigma} \quad (23)$$

$$N = N(\sigma, \theta, \bar{x}, t) = \frac{F(\sigma, \theta, \bar{x}, t)}{\sigma} \quad (24)$$

$$C_g = \frac{1}{2} \left(1 + \frac{2kd}{\sinh 2kd} \right) \frac{\sigma}{k} \quad ; C_\theta = -\frac{1}{k} \left(\frac{\partial \sigma}{\partial d} \frac{\partial d}{\partial m} + \bar{k} \cdot \frac{\partial \bar{u}}{\partial m} \right) \quad (25)$$

$$C_\sigma = \frac{\partial \sigma}{\partial d} \left(\frac{\partial d}{\partial t} + \bar{u} \cdot \nabla d \right) - C_g \bar{k} \cdot \frac{\partial \bar{u}}{\partial s} \quad (26)$$

where $F(\sigma, \theta)$ is the spectral density, d , \bar{k} , \bar{u} are water depth, wave number vector, velocity vector, s is the space coordinate in the propagation direction, θ , the two-dimensional space gradient is ∇ , and m is the spatial coordinate perpendicular to the s direction. The formulations for propagation speed C_g , C_σ and C_θ give a representation of the effect of varying depth and currents on wave propagation. Source functions are: $S = S_{in} + S_{nl} + S_{dis} + S_{bot} + S_{dbs}$, including wind input, nonlinear interactions, white-capping dissipation, bottom friction and depth-limited breaking dissipation. A detailed model description is in Yin et al. (1996).

2.3 The Coupling Procedure

During the simulation process, computed results of interest such as significant wave heights, mean wave periods, directional wave spectra, water surface elevations, current velocities and bottom stresses, with and without the inclusion of coupled interactions can be output by the wave and current models. Following Zhang

and Li (1996), and Mastenbroek *et al.* (1993), a coupling of models was implemented, following the procedure:

- a) The current model is run (15 minute time-steps) using the calculated surface *wind* stress and bottom stress from the previous wave model cycle time step to get elevations and current velocity. This gives *newly* computed elevations and currents, which are passed to the wave model for the next time step computations.
- b) The wave model is run (coarse-grid time-steps, 15 minutes: fine-grid, 5 minutes) using the computed change of water depth (mean water depth plus tide-surge elevation) and inhomogeneous and unsteady currents from the two-dimensional current model to obtain related the wave parameters and wave spectrum.
- c) The bottom stress calculated using the wave spectrum and passed back to the current model.
- d) The calculated bottom stress is calculated and input to the two-dimension current model, which then executes the next time step, resulting in newly computed elevations and currents, to be input to the wave model to repeat the sequence of the computations.

3. NUMERICAL STUDY OF THE HUANGHE DELTA COASTAL AREA

Huanghe Delta coastal area is located in the southwest region of the Bohai Sea. This area has great strategic importance because it is the most important oil production area of the Shengli Oilfield. The fine-resolution grid area, as shown in Figure 1, is the Huanghe Delta coastal area, which is the focus of this study. The purpose of this study is to consider the impacts on bottom stress and current velocities that are due to the wave-current interactions. A secondary objective is to offer a feasibility analysis of the potential for the adoption of a coupled wave-current model to make predictions of wave heights, currents and sea level in this region of the Bohai Sea.

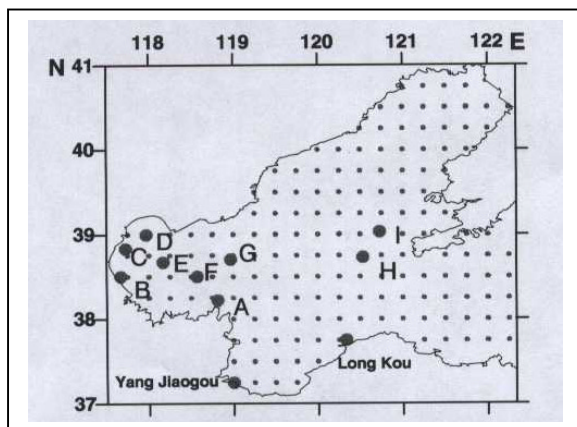


Figure 1. The Bohai and Huanghe Delta coastal area, with buoy location at A •. The location of additional output points B, C, .. and *selected* model grid points are also indicated.

3.1 Case Descriptions

Two storm cases occurred on 22-25 April 1998 and 1-2 April 1999, where measured wave and current as well as sea level data were collected from the buoy site, 38°13'N, 118°19'E, shown in Figure 1. The wind fields were prepared by the Ocean University of Qingdao. Nested coarse- and fine-resolution grids for the wave model are 16'x16' and 2'x2', respectively. See the related paper by Yin *et al.* (2002).

We first consider the wave and current data from the collected the first storm, 22-25 April 1998, at position 38°13'N, 118°19'E indicated in Figure 1. Additional output points are also chosen, at different depths: B(2.8m), C(5.5m), D(10m), E(15m), F(20m), G(25m), H(30m), and I(35m). This allows estimation of the effects of waves on the bottom stress and current velocity. Grids for both wave model and current model are 2'x2', and time steps are 15 minutes. Comparison of results of coupled and uncoupled simulations allows analysis of the effects of waves on the bottom stress and current velocity in the coastal area, in our case specifically the Huanghe Delta coastal region. The following Figures 2-5 give results at point A for wave heights, surface elevations, current velocities and directions, as given from the numerical model.

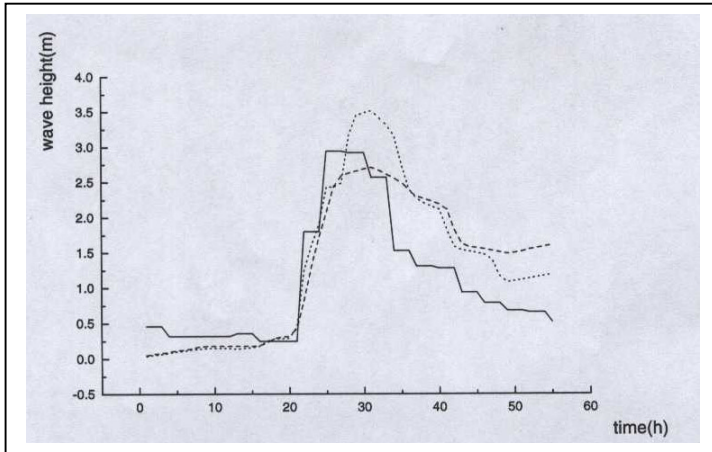


Figure2. Comparisons of simulated and measured wave heights for the 20UTC 22 April 1998- 02UTC 25 April 1998 storm. Measured data — , uncoupled wave model ---, coupled wave-tide-surge model,

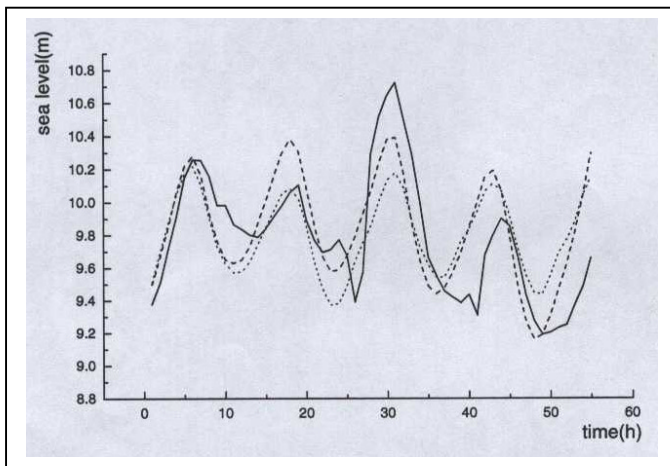


Figure3. Comparisons of simulated and measured sea level for the 20UTC 22 April 1998- 02UTC 25 April 1998 storm. Measured data — , uncoupled tide-surge model ---, coupled wave-tide-surge model,

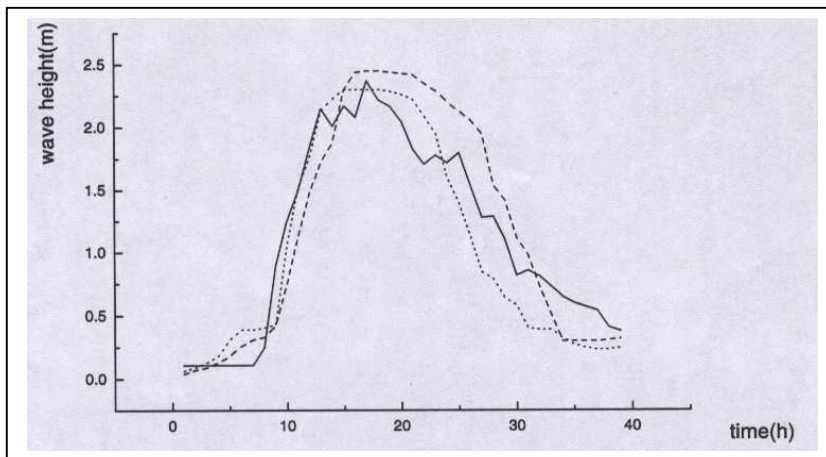


Figure 4. As in Figure 2, for the 00UTC 01 April 1999- 14UTC 02 April 1999 storm.

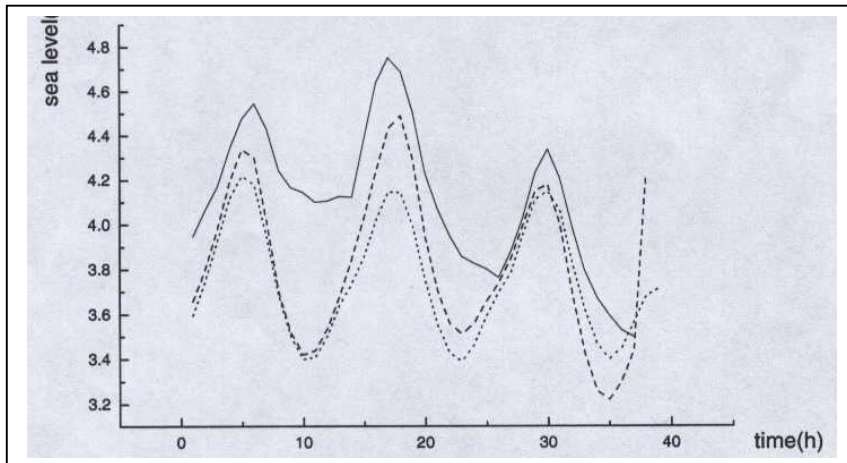


Figure 5. As in Figure 3, for the 00UTC 01 April 1999- 14UTC 02 April 1999 storm.

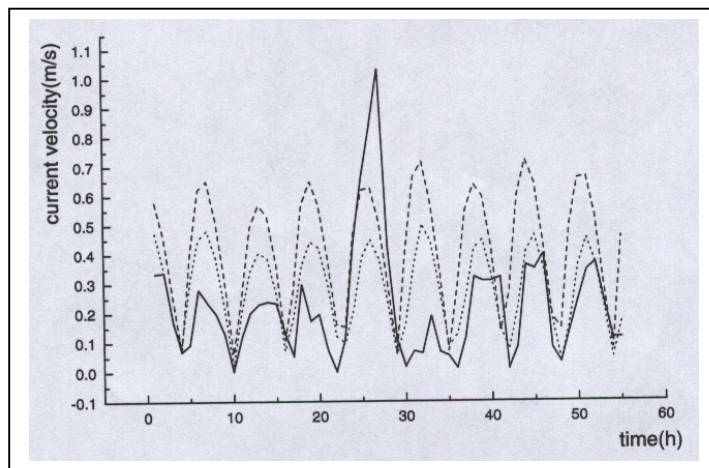


Figure 6. As in Figure 3, comparing simulated and measured current velocities for the 1998 storm.

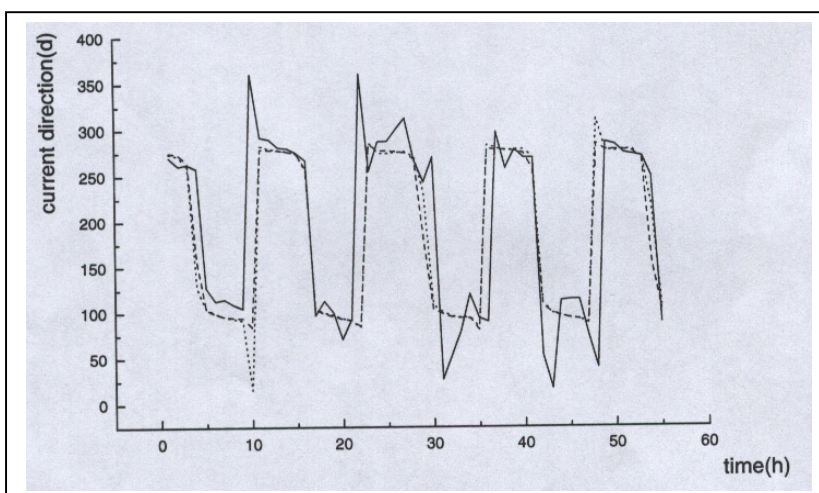


Figure 7. As in Figure 6 for current directions for the 1998 storm. Units are degrees.

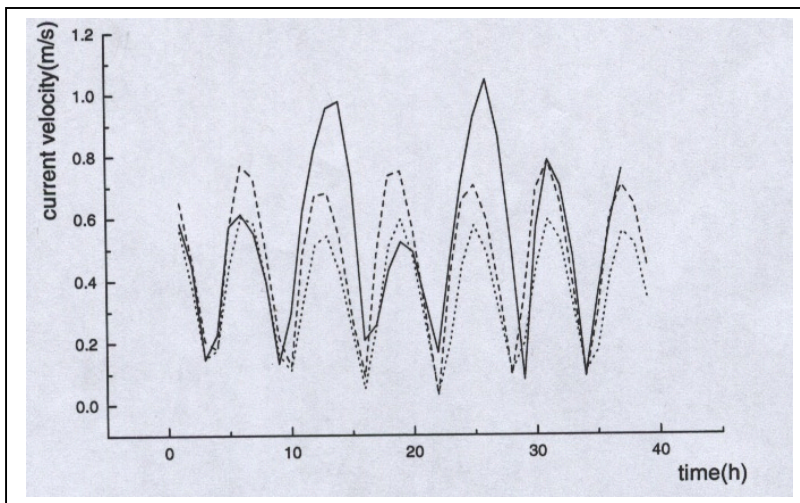


Figure 8. As in Figure 5, comparing simulated and measured current velocities for the 1999 storm.

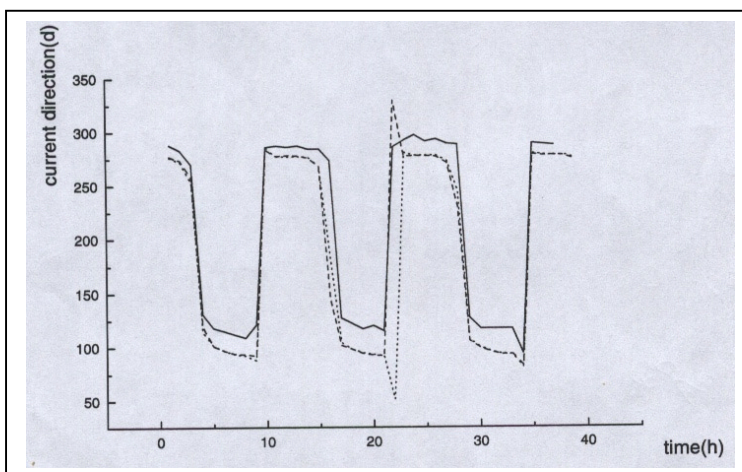


Figure 9. As in Figure 8 for current directions for the 1999 storm.

It follows from Figures 2 and 4 that wave height estimates from the coupled wave-current model are in (very slightly) better agreement with measured values, than those obtained from the uncoupled wave model. From Figures 3, 5, 6-9, we see that estimated sea level and current velocity values from the coupled model are smaller than those obtained from the uncoupled tide-surge model. Corresponding current directions show little difference between the two simulations. These effects can be understood in terms of the wave-bottom effects. The impacts of waves on the current bottom boundary layer are notable: bottom stress is significantly increased due to wave-current interactions. Therefore, a coupled wave-current model is an important consideration because it represents important physical factors and also because it is feasibly practical to implement for operational simulations. Thus it should be the basis for simulating the current velocity and sea level in the near shore region.

Further results are presented in the Appendix, where in Tables 1-2, we give model outputs for bottom stress and current velocity for the output points indicated in Figure 1. These values result from both coupled and uncoupled model simulations, for the 1998 storm. This shows that wave-current interactions in shallow water result in increased bottom stress. Concomitantly, changes in bottom stress affect the current velocity: increased bottom stress give decreased current velocity values. Results from the 1999 storm, are similar. The extent that bottom stress and current velocity changes varies depends on the intensity of the storm.

4. CONCLUDING REMARKS

This paper presents a coastal high-resolution ($2' \times 2'$) coupled wave-current interaction numerical model with explicit consideration of the wave-current interaction bottom stress mechanism. We show that the bottom stress calculated by using a coupled wave-current model is increased, as one would expect, compared with bottom stress values computed by an uncoupled current model. Moreover, the current velocity field is also changed. The extent of changes to bottom stress and current velocities varies with the intensity of the storm. Therefore, it is necessary to develop a coupled wave-current model, taking account of wave-current interactions, particularly for strong storms. From this study, it can be inferred that the adoption of a two-dimensional current model may account for *some* of the wave effects, although it cannot clarify the changes resulting in the vertical current profile. We have shown that the bottom stress effects are large and need to be included. For this reason, it is necessary to develop a three-dimensional current model coupled with a wave model. Thus, we can investigate the impacts of wave-current interactions on the near-bed in shallow seas such as the Bohai Sea.

ACNOWLEDGEMENTS

This paper was partly finished while the first author visited Bedford Institute of Oceanography. We gratefully acknowledge financial supported from NSFC 40076005, Innovation Project KZCX2-202 from the Chinese Academy of Sciences, as well as the USA Office of Naval Research funding to GoMOOS, The Gulf of Maine Ocean Observing System.

REFERENCES

- Davies, A. M., and Lawrence, J., 1994: Examining the influence of wind and wind wave turbulence on tidal currents, using a three-dimensional hydrodynamic model including wave-current interaction. *J. Phys. Oceanogr.*, **24**, 2441-2460
- Christoffersen, J. B., and Jonsson, I. G., 1985: Bed friction and dissipation in a combined current and wave motion. *Ocean Engineering*, **12**, 387-423
- Fang Guohong and Cao Deming, 1990: A 2-D ocean circulation model in Bohai Sea. *Oceanology and Limnology Sinica* (in Chinese), **10(4)**, 300-308.
- Grant, W. D., and Madsen, O.S., 1979: Combined theory wave and current interaction with a rough bottom. *J. Geophys. Res.*, **84**, 1797-1808
- Hsu, S.A., 1986: A mechanism for the increase of wind stress coefficient with wind speed over water surface: A parametric model. *J. Phys., Oceanogr.* **16**, 144-150.
- Jin Zhenghua, Wang Tao, and Yin Baoshu, 1998: The effects of combined wave-tide-surge bottom stress. *Oceanology and Limnology Sinica*, **6**, 604-610 (in Chinese).
- Jonsson, J. G., and Carlsen, N. A., 1976: Experimental and theoretical investigation in an oscillatory turbulent boundary layer. *J. Hydraulic Res.*, **14**, 45-60
- Mastenbroek, C., Burgers, G., Janssen, P.A.E.M., 1993: The dynamical coupling of a wave model and a storm surge model through the atmospheric boundary layer. *J. Phys. Oceanogr.*, **23**, 1856-1866.
- Signell, R.P., *et al.*, 1990: Effect of wave-current interaction on wind-driven circulation in narrow, shallow embayments. *J. Geophys. Res.*, **95**, 9671-9678
- Smith, S. D., R. J. Anderson, W. A. Oost, C. Kraan, N. Maat, J. DeCosmo, K. B. Katsaros, K. L. Davidson, K. Bumke, L. Hasse, and H. M. Chadwick, Sea surface wind stress and drag coefficient: The HEXOS results, *Boundary-Layer Meteorol.*, **60**, 109-142, 1992.
- The WAMDI Group, 1988: The WAM model - A third generation ocean wave prediction model. *J. Phys. Oceanogr.*, **18**, 1775-1810
- Yin Baoshu, Wang Tao, El-Sabh M.I., 1996: A third generation shallow water wave numerical model YE_WAM. *Chinese J. Oceanol. Limnol.*, **14(2)**, 106-112.
- Yin, Baoshu, Perrie, W., Hou Yijun, Lin Xiang, Cheng, Minghua, 2002: The impact of radiation stress in a coupled wave-tide-surge model. *Proceedings of This Workshop*.
- Zhang, M.Y., and Li, Y.S., 1996: The synchronous coupling of a third-generation wave model and a two-dimensional storm model. *Ocean Engineering* **6**, 533-543.

APPENDIX

TABLE 1. Bottom stress at selected points in Figure 1. Coupled model simulations are represented by “Y”, uncoupled simulations, by “N”.

April 22, 1998, hour 20

B		C		D		E		F		G		H		I	
N	Y	N	Y	N	Y	N	Y	N	Y	N	Y	N	Y	N	Y
.089	.095	.231	.248	.230	.248	.585	.616	.642	.672	.539	.555	.677	.700	.659	.670

April 23 “ “ hours 00, 04, 08, 12, 16, 20

.015	.023	.001	.002	.006	.009	.011	.013	.007	.009	.000	.000	.004	.005	.002	.002
.023	.025	.119	.132	.096	.109	.266	.290	.306	.336	.225	.243	.378	.411	.729	.794
.038	.055	.117	.155	.096	.127	.186	.245	.184	.234	.139	.171	.239	.239	.130	.130
.014	.022	.006	.006	.000	.001	.023	.023	.012	.012	.002	.003	.035	.042	.013	.016
.048	.062	.129	.157	.111	.136	.298	.350	.370	.429	.345	.408	.430	.477	.749	.789
.027	.085	.128	.270	.177	.363	.315	.566	.412	.689	.320	.455	.561	.562	.368	.368

April 24 “ “ hours 00, 04, 08, 12, 16, 20

.028	.054	.061	.062	.034	.035	.180	.180	.168	.170	.126	.126	.040	.057	.088	.109
.056	.078	.111	.157	.125	.170	.294	.371	.441	.547	.371	.469	.675	.731	1.18	1.28
.014	.037	.003	.008	.024	.054	.014	.033	.020	.048	.053	.110	.269	.269	.173	.173
.041	.065	.144	.145	.142	.142	.301	.301	.258	.270	.180	.180	.083	.111	.147	.180
.038	.052	.104	.144	.100	.138	.282	.377	.394	.530	.381	.512	.773	.850	1.11	1.18
.015	.026	.033	.034	.001	.002	.020	.020	.001	.004	.002	.008	.229	.229	.131	.131

April 25 “ “ hour 00

.046	.065	.193	.196	.170	.170	.465	.515	.395	.473	.276	.313	.271	.329	.353	.414
------	------	------	------	------	------	------	------	------	------	------	------	------	------	------	------

TABLE 2. As in Table 1, for bottom current velocity in m/s, at selected points in Figure 1. Coupled model simulations are represented by “Y”, uncoupled simulations, by “N”.

April 22, 1998, hour 20

B		C		D		E		F		G		H		I	
N	Y	N	Y	N	Y	N	Y	N	Y	N	Y	N	Y	N	Y
.158	.148	.266	.247	.299	.278	.506	.481	.543	.518	.499	.484	.566	.547	.572	.562

April 23 “ “ hours 00, 04, 08, 12, 16, 20

.113	.074	.035	.021	.077	.050	.082	.070	.080	.063	.035	.014	.033	.032	.042	.036
.086	.076	.201	.181	.203	.179	.353	.324	.393	.358	.338	.312	.443	.409	.617	.566
.150	.104	.214	.161	.239	.182	.393	.298	.405	.319	.367	.299	.308	.303	.267	.267
.096	.062	.028	.028	.059	.012	.061	.061	.045	.045	.052	.037	.186	.153	.121	.096
.100	.078	.219	.180	.233	.191	.407	.347	.461	.398	.434	.368	.483	.436	.595	.564
.157	.050	.187	.089	.223	.109	.346	.192	.396	.237	.397	.279	.496	.495	.437	.437

April 24 “ “ hours 00, 04, 08, 12, 16, 20

.140	.074	.104	.104	.046	.045	.226	.226	.239	.237	.192	.192	.225	.156	.267	.217
.082	.058	.204	.145	.235	.173	.417	.330	.521	.420	.497	.393	.574	.529	.734	.679
.129	.049	.099	.032	.156	.068	.194	.081	.228	.095	.246	.119	.300	.399	.178	.177
.128	.081	.140	.140	.097	.097	.295	.295	.312	.298	.234	.234	.272	.204	.332	.271
.083	.061	.204	.148	.228	.165	.425	.318	.540	.401	.537	.400	.618	.563	.726	.682
.107	.055	.042	.042	.055	.019	.067	.067	.113	.033	.168	.050	.324	.324	.171	.171

April 25 “ “ hour 00

.146	.103	.215	.215	.186	.186	.458	.413	.478	.399	.379	.334	.435	.358	.474	.405
------	------	------	------	------	------	------	------	------	------	------	------	------	------	------	------